General circulation of Lake Superior: Mean, variability, and trends from 1979 to 2006

Val Bennington,[1] Galen A. McKinley,[1] Nobuaki Kimura,[2] and Chin H. Wu[2]

Received 12 March 2010; revised 8 July 2010; accepted 24 August 2010; published 4 December 2010.

[1] Previous observations and modeling studies of Lake Superior have only partly elucidated its large-scale circulation, in terms of both the climatological state and interannual variability. We use an eddy resolving, three-dimensional hydrodynamic model to bridge this gap. We simulate Lake Superior circulation and thermal structure from 1979 to 2006 and consider the mechanisms responsible for the flow. Model results are compared to available direct observations of temperature and currents. Circulation in the lake is primarily cyclonic during all seasons, and a two-gyre structure is sometimes present. Surface circulation patterns in winter mimic wind directions but become organized in summer by the presence of thermal gradients. On the annual mean, nearshore currents are controlled by thermal gradients, while offshore flow is primarily determined by the wind. From a uniform bathymetry simulation, we determine that topographic variations cause small-scale structures in the open lake flow and are critical to the development of nearshore-offshore temperature gradients. The lake exhibits significant variability in current speed and direction on synoptic time scales, but coherent patterns of interannual variability are not found. Long-term trends due to changing meteorological forcing are found. Model results suggest the increase in lake surface temperature (0.37°C/decade) is significantly correlated to increases in wind speed above the lake (0.18 m/s/decade), increased current speeds (0.37 cm/s/decade), and declining ice coverage (−886 km^2/yr).

Citation: Bennington, V., G. A. McKinley, N. Kimura, and C. H. Wu (2010), General circulation of Lake Superior: Mean, variability, and trends from 1979 to 2006, *J. Geophys. Res.*, *115*, C12015, doi:10.1029/2010JC006261.

1. Introduction

[2] Understanding of the mean and variability of the large-scale circulation in Lake Superior is of critical importance to environmental problems such as contaminant and invasive species transport, water quality, and ecosystem analysis and prediction. Mixing, circulation, and temperature determine the availability of light and nutrients for primary productivity, and changes in the thermal structure of the lake should alter locations and timing of phytoplankton blooms. Observations of surface lake partial pressure of carbon dioxide (pCO_2) also suggest the carbon cycle cannot be understood without accounting for spatial heterogeneity in the Lake Superior's physical system [*Urban et al.*, 2005; N. Atilla et al., Observed variability of Lake Superior pCO2, submitted to *Limnology and Oceanography*, 2010]. Lakes are subject to the atmospheric conditions and anthropogenic changes of their larger watersheds, and lake ecosystems may respond more rapidly to changes in the climate system than their terrestrial counterparts [*Williamson et al.*, 2009]. Lake Superior is no exception. Its summer heat content is increasing twice as rapidly as regional atmospheric temperatures [*Austin and Colman*, 2007]. Wind speeds above the lake are also increasing due to a decrease in the lake-atmosphere temperature gradient and are expected to continue to change in warming conditions [*Desai et al.*, 2009].

[3] Lake Superior is the largest lake in the world by surface area and its volume is large enough to hold all of the other Great Lakes combined. The deepest part of the lake exceeds 400 m [*Schwab and Sellers*, 1996], its mean depth is ~150 m, and its water residence time is 178 years [*Quinn*, 1992]. The lake turns over twice yearly, and the entire water column must warm (or cool in winter) to 3.98°C before stratification, because freshwater is densest at 3.98°C. Due to its northern location and great depth, Lake Superior is the coldest of the Great Lakes and often does not stratify until June nearshore and later in the open waters. The lake is completely ice covered about once every 10 years [*Assel*, 2003, 2005], but each year ice forms throughout the nearshore zone. The presence of nearshore ice and otherwise harsh winters have generally precluded wintertime observations of temperature and currents.

[4] There have been a few observations and modeling studies of the mean circulation and interannual variability of circulation in Lake Superior, but overall the system is poorly understood. Published studies on its circulation are based on data that is restricted in space and/or time. The first map of Lake Superior's summer circulation was put together by

[1]Department of Atmospheric and Oceanic Sciences, University of Wisconsin-Madison, Madison, Wisconsin, USA.
[2]Department of Civil and Environmental Engineering, University of Wisconsin-Madison, Madison, Wisconsin, USA.

0148-0227/10/2010JC006261

Harrington [1895] from a bottle drift experiment. He released bottles within the lake and inferred a curved path between the bottle's starting point and where it washed ashore. *Harrington*'s [1895] results exhibited a cyclonic flow around the basin during summer with many bottle paths following the bathymetry. The Federal Water Pollution Control Administration (FWPCA) collected current meter data at point locations throughout the lake during 1966 and 1967. These observations are the most recent lake-wide current observations for Lake Superior. *Sloss and Saylor* [1976] analyzed this data and organized the results into monthly maps of currents at the sixteen summer and nine winter locations. *Beletsky et al.* [1999] summarized the analysis of *Sloss and Saylor* [1976] into two maps, one of mean depth-average summer circulation in the lake and one of the mean depth-average winter circulation. Neither map is intended to represent a long-term mean. Large areas of these maps are empty, particularly in winter, because no current observations exist. Intensive current observations were also taken during the Keweenaw Interdisciplinary Transect Experiments (KITES). Spring throughfall currents and temperatures were measured along the Keweenaw Peninsula during the late 1990s using Acoustic Doppler Current Profilers (ADCP). Current measurements from the KITES project have high temporal and depth resolution but are limited in space to three locations within 21 km (8 km for one transect) of the southern shore.

[5] Given the limited long-term, lake-wide observations, numerical models are valuable tools to fill in the gaps of both time and space. Hydrodynamic modeling of Lake Superior began in the 1970s when *Lam* [1978] simulated the lake-wide currents from June to September 1973 using a 10 km horizontal grid resolution, prescribed lake temperatures, and meteorological winds as forcing. The depth-average large-scale flow of *Lam* [1978] largely agrees with the summer map presented by *Beletsky et al.* [1999], suggesting that depth-average summer flow during 1973 was similar to the summer circulation of 1966 and 1967. *Zhu et al.* [2001] and *Chen et al.* [2001] developed a hydrodynamic model to study the development of the currents along the Keweenaw Peninsula and the effects of heat fluxes on the jet intensification. Their model was lake wide, but the simulations were for summer periods and their analyses focused on currents along the Keweenaw Peninsula. NOAA's Great Lakes Coastal Forecasting System (GLCFS) [*Schwab and Bedford*, 1999] simulates the daily circulation and temperature for each of the Great Lakes, Lake Superior at 10 km resolution. The GLCFS is an excellent tool for water quality predictions. Plots of lake surface temperatures, surface currents, temperature transects, temperature profiles, and water levels for the current date are available online at http://www.glerl.noaa.gov/res/glcfs/. It is unknown by these authors if the many years of hydrodynamic modeling done at GLCFS have been done with a single, internally consistent model. The accumulated years of simulated currents have not been analyzed in the literature. Although hydrodynamic models have been utilized for Lake Superior, studies have not considered the climatological large-scale circulation of the lake or its long-term variability.

[6] In the other Great Lakes, there have been numerical studies that have focused primarily on describing the mean circulation. Lake Michigan's large-scale circulation is best studied. *Beletsky and Schwab* [2008] simulated 10 years of lake hydrodynamics in Lake Michigan during 1998–2007 and found a stable cyclonic depth-integrated circulation during both winter and summer. Weak anticyclonic circulations exist in the far northern and southern regions of the lake. *Schwab and Beletsky* [2003] analyzed the generation of vorticity in Lake Michigan and determined that wind stress curl during winter and heat fluxes during summer are primarily responsible for the pattern of large-scale circulation in the lake. Bathymetry also has an impact on current patterns, but its effect is not as important as wind curl or heat fluxes. Recently, models have been developed for other Great Lakes. *Sheng and Rao* [2006] simulated the circulation of Lake Huron for 1974–1975 using a high resolution, nested grid hydrodynamic model and presented monthly mean circulation and thermal structure of the lake during that time. *Schwab et al.* [2009] presented simulated summer currents in Lake Erie for 1994, and *Prakash et al.* [2007] used a hydrodynamic model to simulate mean circulation patterns and pollutant transport in Lake Ontario.

[7] In this paper, we simulate the thermal structure and circulation of Lake Superior from 1979 to 2006. This is the longest single Great Lake simulation to date. Modeled temperatures and currents are compared to available observations. Seasonal maps of the climatological circulation are created for surface, depth average, and below 50 m depths. Variability in depth-average currents at nine open lake stations is examined and summarized in current rose plots. We address the following questions. What are the climatological patterns of the lake's circulation? How much does the current direction change from year to year? Do winds and heat fluxes control Lake Superior's circulation, as in Lake Michigan, or does the bathymetry have a greater control on flow? How has the lake circulation and thermal structure changed over the last 3 decades?

[8] The paper is organized as follows. Section 2 includes a description of the hydrodynamic model and a comparison of model results to observations. The climatology of Lake Superior's circulation is presented in section 3.1, and mechanisms of the lake circulation are examined in section 3.2. We discuss lake-wide trends in section 3.3. Discussion and conclusions are presented in section 4.

2. Model

2.1. Physical Model

[9] Lake Superior's large volume and long residence time (178 years) [*Quinn*, 1992] make it an appropriate water body to study with a fixed volume numerical model. We use the MIT general ocean circulation model (MITgcm) [*Marshall et al.*, 1997a, 1997b] configured to the bathymetry of Lake Superior [*Schwab and Sellers*, 1996]. The MITgcm has been used to simulate circulation in water bodies of all sizes [e.g., *Dutkiewicz et al.*, 2005; *Dororstkar et al.*, 2010; *Liu and Lamb*, 2010; *Querin et al.*, 2006]. The model resolves eddies and has a uniform horizontal resolution of 2 × 2 km. The model uses a z coordinate system of 28 vertical layers. The top 50 m have finest vertical resolution, with layer thicknesses of 5 m. Vertical resolution gradually becomes coarser with depth to a thickness of

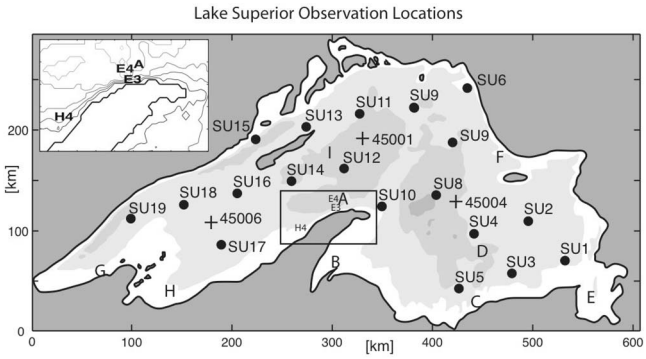

Figure 1. Locations of observations in Lake Superior used for model evaluation. Solid circles indicate the 19 open lake EPA stations (SU1–SU19). Three crosses show locations of three surface buoys operated by NOAA. A–I are locations of current measurements from *Sloss and Saylor* [1976]. E3, E4, and H4 are ADCP locations during the KITES experiment. Shaded contours every 100 m. Inset of boxed region along the Keweenaw Peninsula. Isobaths within inset every 50 m.

33.7 m at 322 m depth. The model setup uses the hydrostatic approximation. The *Smagorinsky* [1963] horizontal diffusivity scheme and the K Profile Parameterization (KPP) vertical mixing scheme [*Large et al.*, 1994] simulate the effects of subgrid-scale processes.

[10] A bulk formula atmospheric module is used to calculate momentum exchange and heat fluxes between the atmosphere and lake, dependent on atmospheric stability. Model evaporation is a function of local winds, lake surface temperature, and atmospheric humidity. The rate of evaporation is modified by the atmospheric stability. We do not include precipitation in the model. Ice cover data from NOAA [*Assel*, 2003, 2005] is applied as a fractional mask to each grid cell at daily resolution, as done in the oceanographic work of *McKinley et al.* [2004] and *Dutkiewicz et al.* [2005]. The presence of ice alters lake albedo and prohibits a fraction of the evaporation, heat, and momentum exchange. This fraction is equal to the fraction of the grid cell that is ice covered. If a grid cell is 40% ice covered, 60% of the ice-free heat fluxes and momentum exchange is assumed. Temporal increases/decreases in fractional ice coverage create a heat flux to/from the lake. For this purpose, lake ice is assumed to have a constant thickness of 0.25 m when present.

[11] The model is forced with 3 hourly winds, downward shortwave and longwave radiation at the surface, air temperature, and specific humidity from the North American Regional Reanalysis (NARR) [*Mesinger et al.*, 2006] between 1979 and 2006. This forcing product has a uniform horizontal resolution of 32 km. NARR is the only dynamically consistent, historical, and freely available public data set that provides meteorological conditions over all of North America at 3 hourly and 32 km spatial resolution between 1979 and the present (section 1 of Text S1).[1]

[12] The time step of numerical integration is 200 s. The physical model is spun up for 5 years using 1979 forcing before the model is run for 1979–2006. After the first year of the spin up, the next 4 years are identical, indicating model drift is insignificant. For the entirety of the analysis, summer is June–September (JJAS), to be consistent with the circulation maps presented by *Beletsky et al.* [1999].

2.2. Model: Observation Comparisons

[13] To evaluate the model simulation, we utilize the available temperature and current observations throughout the lake.

2.2.1. Model-Observation Temperature Comparisons

[14] The National Data Buoy Center (NDBC) observes surface water and meteorological conditions on Lake Superior between April and November at the three open lake buoy stations shown in Figure 1. Buoys 45001, 45004, and 45006 became operable in 1979, 1980, and 1981, respectively. In Figure 2, we show model surface temperature at the three buoy locations during 2000 and 2004. Modeled surface temperatures capture both the seasonal cycle and synoptic variability in surface temperatures observed at the three buoys during 2000. In 2000, root mean square error (RMSE) at buoys 45001, 45004, and 45006 are 1.14, 1.14, and 1.54°C, respectively. During 2004, modeled surface temperatures are higher than observed because the model stratifies earlier than in the data. In 2004, the RMSE at buoys 45001, 45004, and 45006 are 2.78, 3.05, and 2.9°C, respectively. The model generally warms too early in spring and does not cool as rapidly as observed; however, the shapes of the seasonal cycles at the three buoys are consistent with the spatial and temporal heterogeneity seen in the observations. The model captures cooling and warming events on synoptic time scales recorded by the buoys, suggesting the model adequately represents physical processes but has a warm bias. During 2004, temperatures during August and September were below the 28 year mean of 12.1, 12, and 14.3°C at buoys 45001, 45004, and 45006, respectively. The summer of 2000 was warmer than average.

[15] For the entire 28 year period, model RMSE at buoys 45001, 45004, and 45006 are 3.2, 3.0, and 3.4°C. During years with above average temperatures during August and September (warm years), model RMSE are 2.7, 2.4, and 3.1°C; RMSE during colder years (August and September temperatures below mean) are 3.7, 3.7, and 3.8°C. Although modeled temperatures are generally warmer than observed at the buoys, interannual variability in modeled summer temperatures at the buoys are highly correlated with observations ($r^2 = 0.73$). The RMSE for all years at the buoy locations is provided in Table S1, and summer average temperatures at buoy locations in the model and data are shown in Figure S1.

[16] The Environmental Protection Agency (EPA) has been sampling the physical and chemical characteristics at ~8 depths within the water column at nineteen open lake stations in Lake Superior (Figure 1) twice each year since 1992, usually in April and August. The sampling depths are not consistent from year to year or between stations, so we compare model temperatures to EPA observations (Figure 3) at the EPA depths closest to two depths (surface, below 75 m) in April and at three depths (10, 20, below 75 m) in summer, using all available years on GLENDA, the EPA's

[1] Auxiliary materials are available in the HTML. doi:10.1029/2010JC006261.

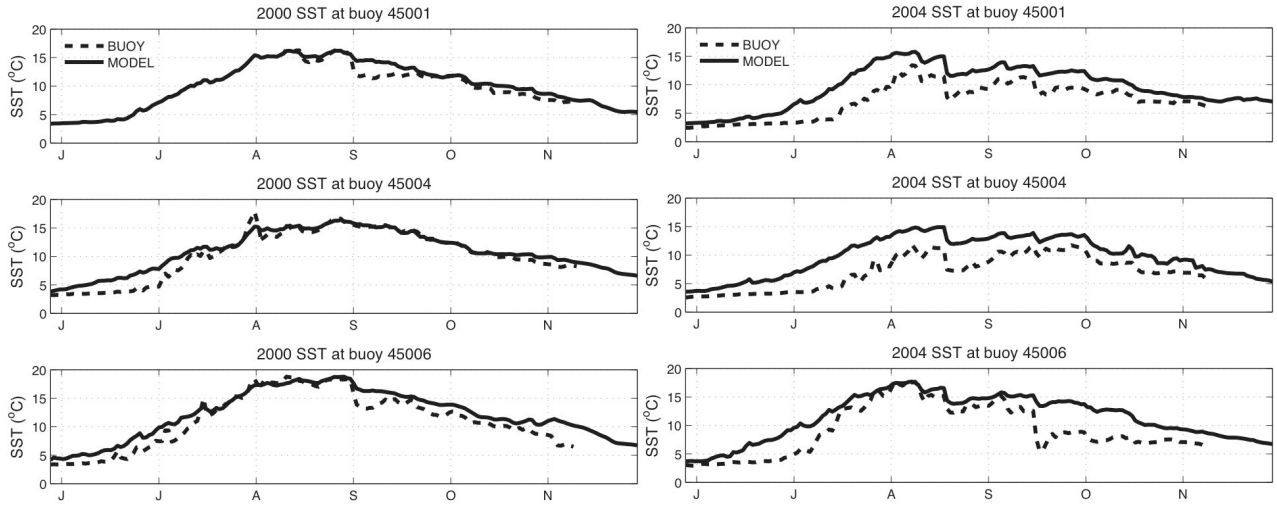

Figure 2. Daily average modeled and observed lake surface temperatures at the three NDBC buoy locations during (left) 2000 and (right) 2004. The year 2000 was a year of above average lake temperatures, and 2004 temperatures were below the 28 year average.

searchable data archive website (http://www.epa.gov/glnpo/monitoring/data_proj/glenda/glenda_query_index.html).

[17] During April, the model overestimates surface temperatures with a root mean square error (RMSE) of 1.06°C at the surface and 0.77°C below 75 m. Station to station and year-to-year variability in modeled temperatures correlate to observations with $r^2 = 0.6$ at the surface and $r^2 = 0.42$ and below 75 m in April. The model is better able to capture observations above 2°C, so the scatterplot is overall flatter than the one-to-one reference line. Modeled lake surface temperatures are warmer than observations during summer (RMSE = 3.2°C), but the model captures the spatial and interannual variability present in EPA observations with an $r^2 = 0.83$. The modeled thermocline is not as sharp as observed, thus modeled temperatures are too warm within the thermocline at 20 m (RMSE = 5.1°C). Water in the hypolimnion (below 75 m) is captured well in the model, with a RMSE of 0.3°C and r^2 of 0.97. The model warm bias may be partially explained by a warm bias in the 10 m air temperature forcing described below. Even with the known

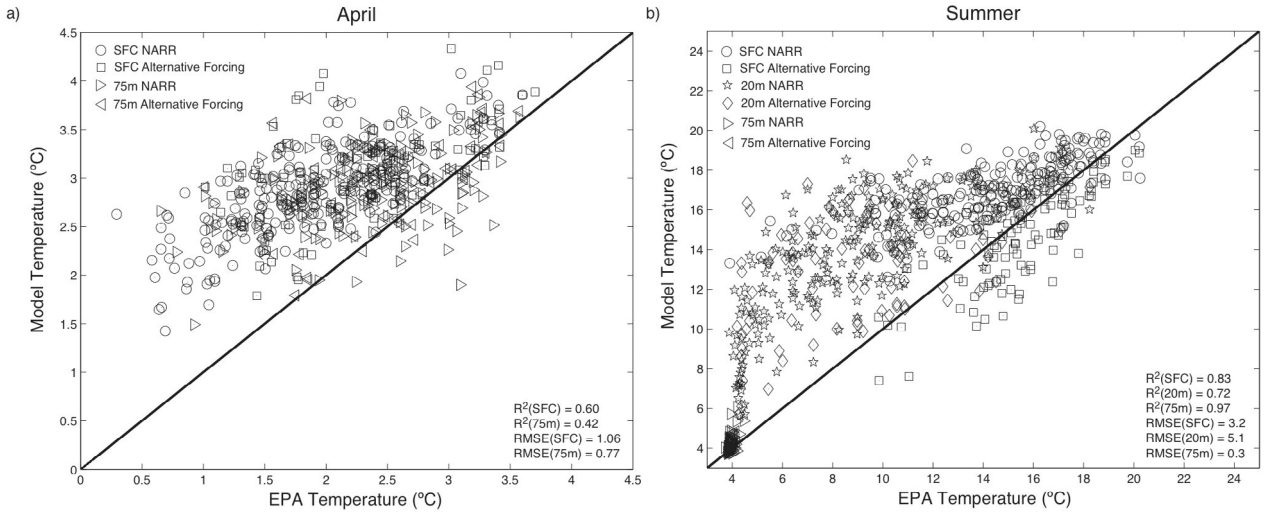

Figure 3. Model daily average temperature plotted against instantaneous temperature measured at the 19 EPA stations between 1992 and 2006 during (a) April and (b) summer. Model results when forced with alternative forcing (see auxiliary material) are included on the scatterplots. Summer sampling primarily done during the month of August. Model temperatures compared to sample temperature at depths nearest the surface and below 75 m in April. In summer, model temperatures compared to sampled temperatures nearest the depths of 10, 20, and below 75 m. One-to-one line shown on both Figures 3a and 3b for ease of comparison. R^2 and RMSE are shown for modeled temperatures when forcing the model with atmospheric conditions of the NARR product.

bias, the model captures observed variability, with colder observed years being colder modeled years, just not as cold as observed.

2.2.2. Warm Bias in NARR Forcing

[18] The North American Regional Reanalysis Project is a long-term, 32 km horizontal resolution climate product for the North American region. Air temperatures above Lake Superior have a warm bias in NARR. When compared to air temperatures observed at the NDBC buoy locations, NARR forcing has a RMSE of 2.4°C during April. NARR 10 m air temperatures at the NDBC buoy locations on Lake Superior have large RMSE (4–7°C) and a warm bias during May–July (Figure S2). NARR air temperatures above the lake are biased warm except during the warmest years.

[19] To determine atmospheric conditions above the Great Lakes, the North American Regional Reanalysis Project sets lake surface temperatures to a spatially heterogeneous climatology of its seasonal cycle (F. Mesinger and D. Schwab, personal communication, 2009). Interannual variability in observed lake surface temperatures are not utilized. Once lake temperature reaches 3.98°C, the lake stratifies and surface temperatures rapidly increase. Due to averaging, the climatology of lake surface temperatures is significantly warmer than observed during the spring and early summer of the cooler years; thus, boundary conditions for the atmospheric product are too warm during cooler years. A lake that is warmer than observed will cause air temperature above the lake to be warmer than observed in the atmospheric product. The warmer waters may also decrease the atmospheric stability above the lake in spring, when lake temperatures are cooler than air above the lake. Boundary layer parameterizations in the NARR atmospheric model may also cause spring and summer air temperatures to be too warm.

[20] The warm bias in NARR air temperatures causes the model to be too warm in spring and summer. The larger summer heat content means that the heat loss from the lake during winter must be greater than observed for the lake to cool to observed temperatures. This effect and the lack of an explicit lake-ice model contribute to model error during April. If the model does not cool to zero degrees in all years before the ice mask is applied, the presence of ice impedes lake cooling and traps some heat over winter. This can modify local surface temperatures by up to one degree during spring.

[21] Although the product has a known warm bias, winds in NARR are similar to winds in an alternative forcing, interpolated from meteorological observations (not shown). NARR winds produce currents in agreement with observations (section 2.2.3) and result in the same large-scale circulation as when using the alternative forcing. The trend in wind speed above Lake Superior (0.18 m/s/decade) is comparable to buoy and satellite observations (0.51 m/s 1985–2008 [*Desai et al.*, 2009]). The trend in atmospheric temperatures above the lake is also present in the NARR product. Thus, model results will be warmer than observations but is responding to realistic changes in atmospheric conditions.

2.2.3. Model-Observation Current Comparisons

[22] No lake-wide multiyear current observations exist in Lake Superior. Modeled surface circulation during summer is qualitatively similar to the lake-wide circulation deduced by *Harrington*'s [1895] bottle drifter experiment. Lake-wide depth-average currents were observed by the FWPCA during the late 1960s. We determine the speed and direction of depth-average flow at nine locations around the lake, consistent with current observation locations depicted by *Sloss and Saylor* [1976]. We average to 150 m, because FWPCA instrumentation did not exceed this depth. Figure 4 depicts the daily speed and direction of depth-average flow at the nine stations during summers of 1979–2006. Figures 4a–4i correspond to the locations A–I shown in Figure 1. Daily depth-average current direction and speed are depicted in the current roses for each location A–I. Bar direction indicates direction *toward* which current flows. Length of bar indicates percentage of summer days (1979–2006) that daily average flow is in that direction. Color of bar indicates speed of flow. Flow in one direction may have many colors, indicating percentage of days that daily average flow was both in that direction *and* with that speed. Separate arrow indicates direction *toward* which current flow was observed by the FWPCA, as summarized by *Beletsky et al.* [1999]. Color and number at end of arrow indicate mean speed of the observed flows [*Sloss and Saylor*, 1976]. Due to instrumentation failures, FWPCA data does not span the entire depth and season at all nine selected locations. Exact latitude and longitude coordinates are also not available for the direct observations, so we selected the model grid cell of the observations by matching the bathymetry to published figures of *Sloss and Saylor* [1976].

[23] We first note that modeled flows are generally in good agreement with current speed and direction observed by the FWPCA in summer. At locations A, B, C, E, F, and H, modeled currents are in the same direction as observed. At location D, modeled current direction is highly variable and mean observed flow suggests currents toward the northwest. At location G, the model shows a bimodal distribution of direction, and so only agrees with the observed mean for about half of the days of summer. Just east of Isle Royale, at location I, simulated currents are generally more southward than those observed. Modeled flows are highly variable, and only at locations A and C are daily average currents consistently in one direction for more than 20% of the summer. When considering both direction and speed, less than 5% of summer days have the same direction (±5°) and speed (±0.5 cm/s) at every location except C (<10% of summer days at C).

[24] Current observations with high temporal resolution are only available nearshore during the late 1990s. In spring through winter of 1998 and 1999 during the Keweenaw Interdisciplinary Transport Experiments (KITES), Acoustic Doppler Current Profilers (ADCPs) were stationed offshore along the Keweenaw Peninsula (Figures 1 and 5). The instruments recorded zonal and meridional velocities and temperature throughout the water column. In Figure 5, we compare modeled and observed current velocities and temperature through the water column at station H3 from May to December 1998. The model is able to capture the seasonal cycle of temperature, cooling events, and the magnitude and direction of horizontal velocities unique to the station. The model is able to replicate the observed spatial and temporal heterogeneity, and captures temperature and velocity patterns. Modeled currents rapidly change from baroclinic to barotropic (and back) and are able to completely reverse

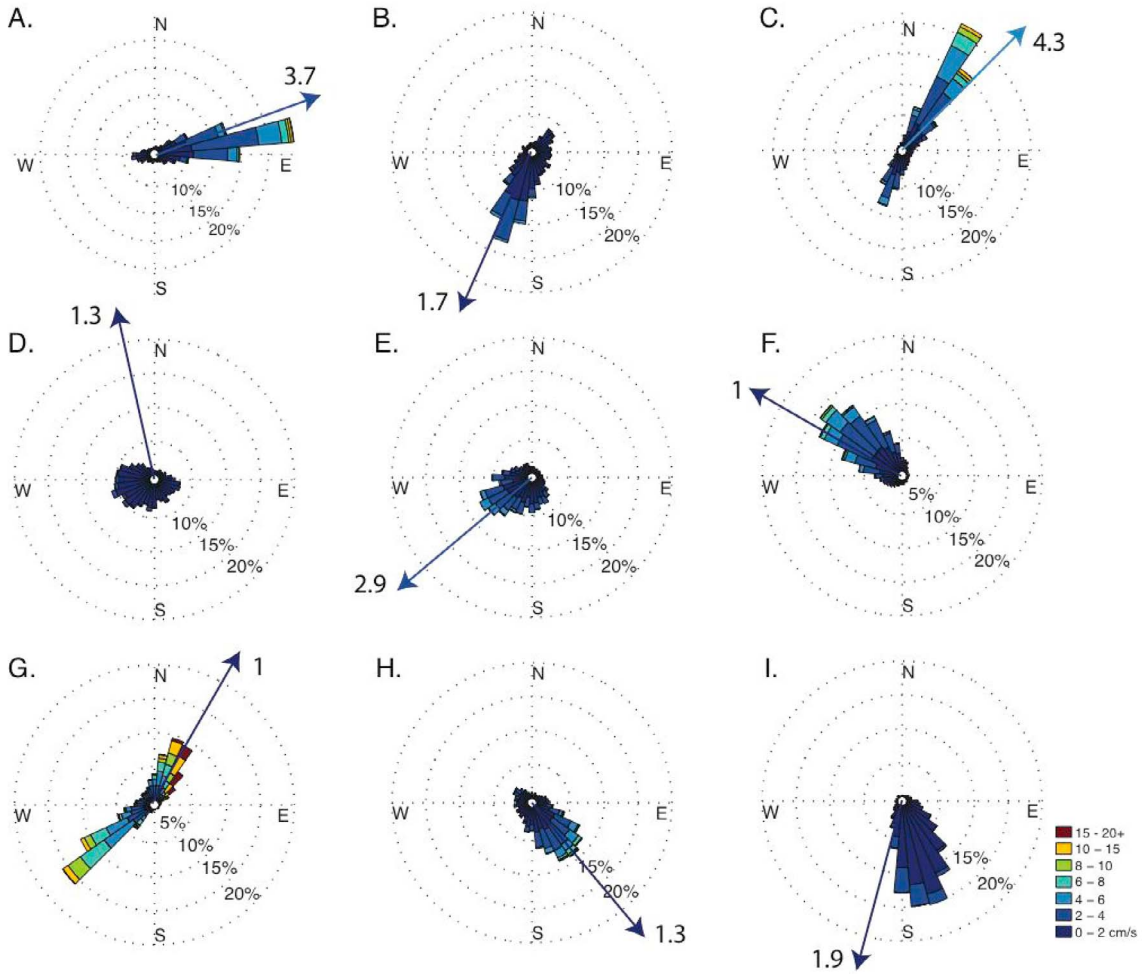

Figure 4. Figures 4a–4i correspond to the locations A–I shown in Figure 1. Daily depth-average current direction and speed are depicted in the current roses for each location A–I. Bar direction indicates direction *toward* which current flows. Length of bar indicates percentage of summer days (1979–2006) that daily average flow was in that direction. Color of bar indicates speed of flow. Flow in one direction may have many colors, indicating percentage of days that daily average flow was both in that direction *and* with that speed. Separate arrow indicates direction *toward* which current flow was observed at that location during 2 years during the 1960s, as summarized by *Beletsky et al.* [1999]. Color and number at end of arrow indicates mean speed of the observed flows [*Sloss and Saylor*, 1976].

direction on daily time scales as observed, capturing the transient nature of local flow in Lake Superior. It is also able to capture station-to-station and year-to-year variations (Figures S3 and S4). The model over predicts maximum summer surface temperatures and begins to stratify prematurely in spring, consistent with NARR's warm bias (section 2.2.2). Heat also penetrates deeper in the model than in the data because the thermocline is too deep, in part due to lack of colored dissolved material in the model, which has been found to increase the attenuation of light within the water column in the global ocean [*Anderson et al.*, 2007].

[25] In summary, although the model has a warm bias due a biased meteorological forcing product, the model captures the spatial and temporal (daily, seasonal, and interannual) variability in the thermal structure and circulation seen in observations. Warming and cooling events driven by the passing weather systems occur in the correct locations and at the correct time, as seen in the buoy measurements of lake surface temperature. The model is unable to capture the coldest temperatures during the coldest years but replicates warmer years well, and modeled surface temperatures correlate well with EPA observations (r^2 = 0.83) and lake surface temperatures at the open lake buoys (r^2 = 0.73). Under influence of a warming climate, as experienced between 1979 and 2006, trends in temperature should be dampened in our results given the enhanced warm bias during cold years. However, the trend in NARR wind speed above the lake (0.18 m/s/decade) is comparable to observations (0.51 m/s 1985–2008 [*Desai et al.*, 2009]). Thus, the model should capture trends in thermal structure

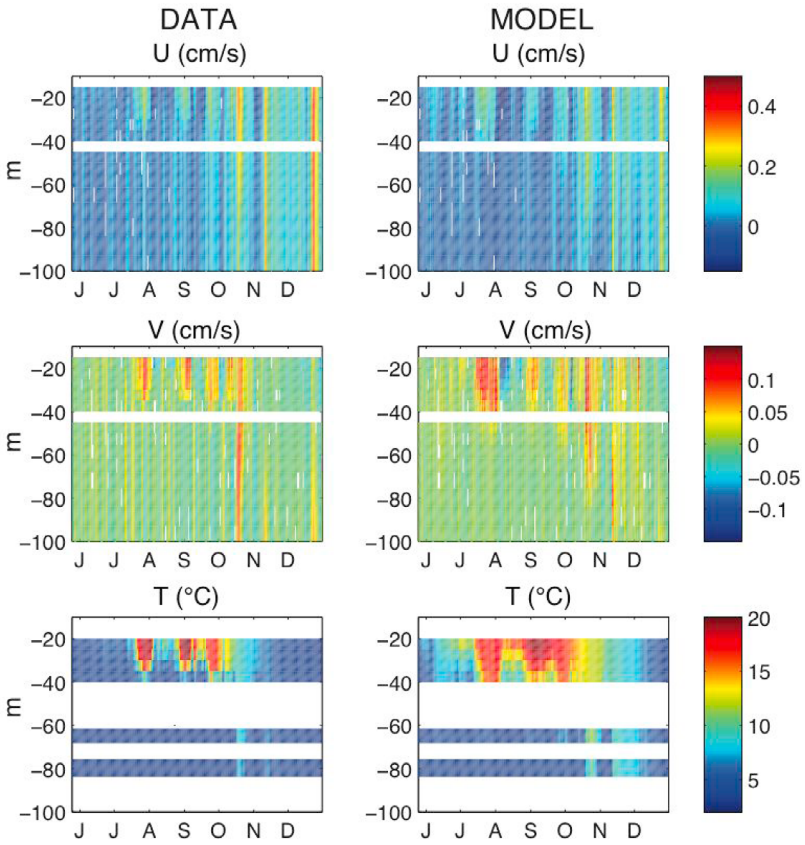

Figure 5. Zonal velocity (U), meridional velocity (V), and temperature (T) at ADCP location H3 during the summer of 1998. (left) Data and (right) model are shown. Data and model plotted versus depth (m) and time (day). Month denoted on first day of the month. Data averaged within model layers. For ease of comparison, model layers with no ADCP measurements are left blank for both data and model.

and circulation due to this increase. The directions and magnitudes of daily and seasonal observed currents are captured by the model, and we believe the model is an adequate tool to analyze the circulation and long-term changes in lake thermal structure.

3. Results

3.1. General Circulation

[26] Figure 6 shows model results for the general circulation averaged over 1979–2006 during winter (DJFM) and summer (JJAS) in the top 15 m, below 50 m, and throughout the entire water column. Colors depict the average water temperature within the same columns. Animation S1 provides daily resolution of temperature and currents for these three layers.

[27] During winter, winds are primarily from the north, and horizontal gradients in water temperature are small. Temperature increases with depth to just under four degrees below 50 m. The water column can stratify, with coldest water at the surface, but currents are primarily barotropic during winter, indicated by the similarity of surface currents to those at depth. Currents are southward in the western arm of the lake. There is a return flow toward the northeast along the Keweenaw Peninsula. A temperature gradient exists from near to offshore along the peninsula with colder waters nearshore. This alone would support a flow toward the southwest if the resulting pressure gradient force was balanced by the Coriolis force (thermal wind). Thus, the northeast flow indicates dominance by the wind. Some northward flow exists in the eastern and central parts of the lake during winter, where there are two rough cyclonic cells just east and north of the Keweenaw Peninsula. When the model is run at coarser (10 km) horizontal resolution, the circulation pattern is smoothed and the gyres can be more easily viewed by the reader (Figure 7).

[28] During summer, there are significant near to offshore temperature gradients and winds from the southwest (Figure 6). Warmer waters are along the coastlines, since shallower water heats more rapidly. We choose to separate the flow above 15 m and below 50 m so that flow in the variable depth of the thermocline zone does not confuse the interpretation. In contrast to winter surface circulation, summer flows above 15 m do not mimic winds. The circulation is largely cyclonic, i.e., the flow pattern is counterclockwise along the eastern coastlines. Flow diverges when it reaches Isle Royale, and there is a southward flow to the Keweenaw Peninsula. The flow east of Isle Royale may be viewed as a single cyclonic surface gyre. The western arm is warmer than the eastern arm. Circulation is

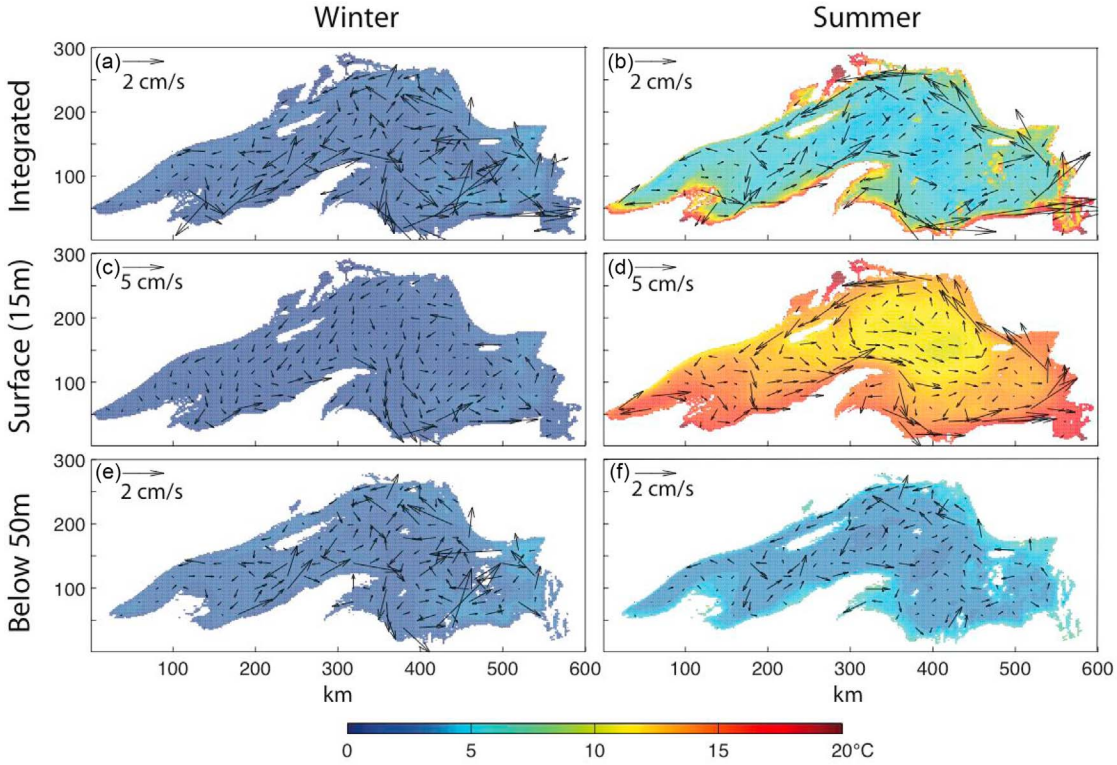

Figure 6. Depth-average currents and column temperature during (a) winter (DJFM) (1979–2006) and (b) summer (JJAS) (1979–2006). Mean currents and column temperature within the top 15 m of the water column during (c) winter and (d) summer. Mean currents and temperature of the water column below 30 m during (e) winter and (f) summer. Note change in current scale for surface flows.

still primarily counterclockwise along the coastlines, but the southwesternmost region of the lake, by the mouth of the St. Louis River, is anticyclonic. Summer circulation is baroclinic, and small-scale structures are omnipresent below the thermocline. Two cyclonic cells follow along the isobaths. A cell exists just east of the Keweenaw Peninsula, and a second, smaller, cell exists north of the Keweenaw Peninsula and east of Isle Royale. Summer depth-average flows are strong and counterclockwise along the coastlines. Flow is cyclonic everywhere except in the far southwestern arm, and there is weaker flow along the 200 m isobaths within the two cyclonic gyres.

3.1.1. Current Speed

[29] Lake-wide mean current speeds peak in October and November (2.8 cm/s) and decay over winter, reaching a minimum during late May (0.7 cm/s). Current speeds are relatively constant between March and May. Although wind speeds are greatest in winter, thermal gradients within the lake decrease and increased ice coverage decreases the transfer of momentum to the lake. The annual average of lake-wide depth-average current speed is 1.5 cm/s. Fast coastal currents begin to develop in June after slowing throughout winter and spring, and coastal currents reach maximum mean velocities of over 5 cm/s during October and November (>15 cm/s in top 15 m). Open lake current speeds are weakest during May and June and strongest in October and November (2.5 cm/s), when an ice-free lake begins to experience increasing winds. Offshore flows remain above 2 cm/s until January, when they begin to significantly slow because of ice coverage. (Figure S5). Surface velocities (top 15 m) show the same seasonal cycle and structure as depth-average velocities throughout the lake, but reach a maximum lake-wide mean speed of 7.4 cm/s in October and weakest velocities (2–3 cm/s) from March to May.

3.1.2. Variability

[30] In Figure 4, we depict direction and speed of summer currents for all years on a single plot. Selecting any individual year during the model simulation results in current roses with nearly identical distributions of current direction at all nine locations; thus interannual variability in summer depth-average currents appears to be minimal. However, variability on daily and synoptic time scales is significant, as all current roses exhibit spread in current speed and direction. These distributions are also robust to alternative choices of "summer" months. Daily variability of currents is therefore more significant than interannual variability, and when considering speed, each location can be understood as having a probability distribution function of currents during summer.

[31] We conclude that the mean current direction depicted by *Beletsky et al.* [1999] are generally representative of the flow for nearly all days of summer at locations A, B, F, and H. Current directions at locations C, D, E, and G are best understood as probability distributions. While flow at location C is most often toward the northeast, twenty

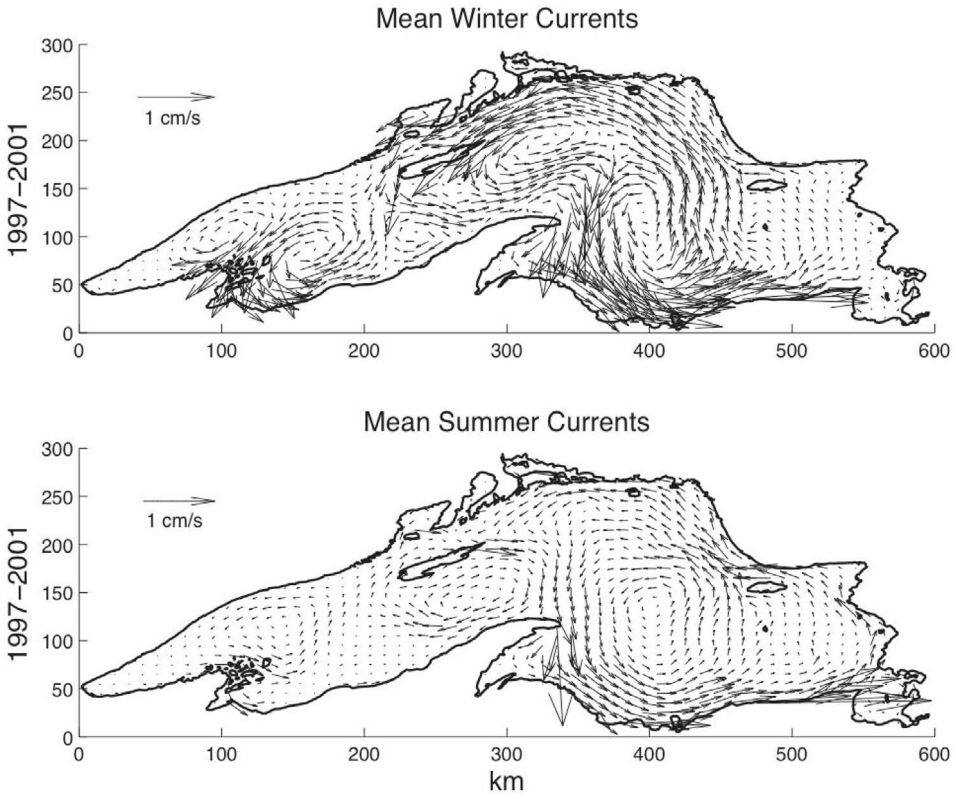

Figure 7. Depth-average currents during (top) winter (DJFM) and (bottom) summer (JJAS) of 1997–2001 from model simulation with a 10 km horizontal grid resolution. Current speed indicated by arrow length.

percent of the time currents are weaker and toward the southwest. Here, flows may enter the cyclonic cell when going toward the northeast. Near the eastern part of the same cell, depth-average currents at location D are best described as weak and frequently westward. Significant spread in direction near Sault Saint Marie at location E is also present. In the far western arm, at location G, currents are bimodal and stronger than averaging observations would suggest. Flows are toward the southwest just as often as toward the northeast, so mean currents only tell part of the story. Even currents along the Keweenaw Peninsula (location A) can weakly reverse direction when winds are able to overcome the temperature gradient [*Zhu et al.*, 2001].

3.2. Current Mechanisms

[32] What controls the current speed and direction? In Lake Michigan, *Schwab and Beletsky* [2003] find that lake-wide vorticity is primarily generated by vorticity in wind stress during winter and baroclinic effects during summer. Vorticity generated by the bottom topography is a second-order effect. Are the mechanisms similar in Lake Superior?

[33] For wind-driven currents we expect that transport within the Ekman layer to be 90° from wind stress. For thermally driven flows, we expect currents to be geostrophic and thus along isotherms, with colder water to the left. To determine how much thermal gradients contribute to both the direction and speed of currents, we correlate daily anomalies of local temperature gradients in the zonal direction with daily anomalies in current speed in the meridional direction (r_{mt}). We correlate daily anomalies of the local temperature gradient in the meridional direction with daily anomalies in the current speed in the zonal direction (r_{zt}). We present the spatial distribution of the geometric mean (r_g) of these correlations (equation (1)) in Figure 8 (top)

$$r_g = \sqrt{|r_{zt} \times r_{mt}|}. \quad (1)$$

[34] A geometric mean of 1 indicates a perfect correlation of wind stress anomalies and currents in both zonal and meridional directions. Correlations between temperature gradients and currents may be underestimated due to the use of local temperature gradients.

[35] Similarly, we would like to know how significant an effect wind stress has on local currents. We compute the geometric mean of correlations between daily anomalies in wind stress in the zonal direction with daily current anomalies in the meridional direction and correlations between daily anomalies in wind stress in the meridional direction with daily current anomalies in the zonal direction. The resulting geometric mean of these correlations is shown in Figure 8 (bottom). We integrate to 25 m, because the Ekman depth is dependent on the eddy flux of momentum and varies in both time and space. Integrating to 50 m does not significantly alter the results or conclusions.

[36] Figure 8 clearly shows that near surface flows in the open lake and immediately onshore are significantly

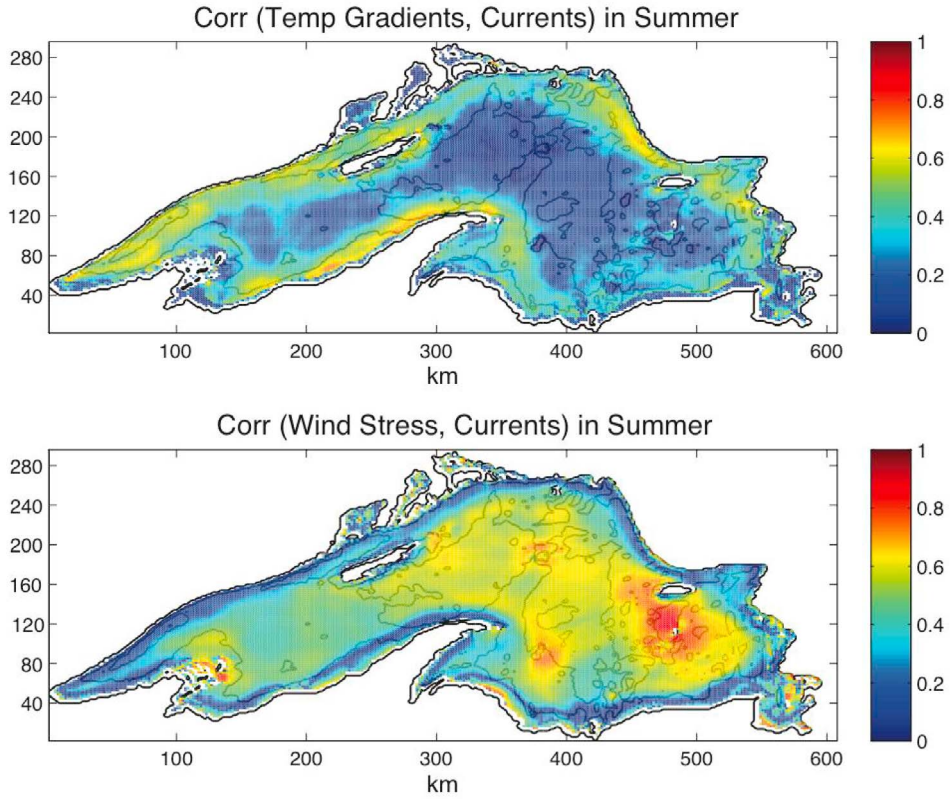

Figure 8. (top) Geometric mean of (1) correlation between daily summer zonal temperature gradient anomalies and meridional current anomalies (depth average to 25 m) and (2) correlation between daily meridional temperature gradient anomalies and zonal current (depth average to 25 m) anomalies during summer. A geometric mean of 1 corresponds to a correlation of 1 for both (1) and (2). (bottom) Geometric mean of (1) correlation between daily summer zonal wind stress anomalies and meridional current (depth average to 25 m) anomalies and (2) correlation between daily summer meridional wind stress anomalies and zonal current (depth average to 25 m) anomalies.

correlated with the wind stress, but currents within the coastal jets are steered along isotherms and are faster flowing when temperature gradients increase. A change in winds is accompanied by a change in surface flows during the same day in the open lake and within a couple kilometers of the shore. Similarly, if a temperature gradient from near to offshore is observed, the pattern and speed of the coastal jets may be inferred. We show summer correlations, because they are strongest, but annual correlations show the same pattern. The correlations were computed for lags up to one week, but correlations were strongest for both wind and temperature gradients with a lag of zero. Thus, changes in wind or temperature gradient translate into a change in surface currents on the same day.

[37] We cannot decompose depth-average flows in the same manner, since we do not expect a change in winds to result in currents to change at a 90° angle below the Ekman Layer. However, the pattern is identical when we correlate daily anomalies in wind speed and depth-average current speeds and the magnitude of the thermal gradient and depth-average current speeds. Winds are the dominant current mechanism in the open lake and immediately onshore, and temperature gradients control flows nearshore. This finding is consistent with sensitivity studies in a model of 10 km horizontal resolution, in which the model is run without wind, without heat fluxes (barotropic), and with a spatially averaged wind field (no curl) (section 2 of Text S1 and Figure S6). Thus, wind is a first-order control of circulation patterns all year, but temperature gradients in summer are the first-order control of near-coastal flows.

[38] Although it is apparent winds are important to the circulation pattern, the cyclonic gyres are also coincident with lake bottom topography. We would like to know if the wind-induced pattern would differ without the topographic gradients. To consider this effect, we run the model with a uniform, flat bathymetry of the mean lake depth, such that lake volume is the same as in real bathymetry simulations. Lake coastlines remain unchanged. In Figure 9, we present monthly average flows and vorticity for January and June 2006 from the flat bottom and realistic topography runs. Bathymetry significantly changes the horizontal temperature structure of the lake. Shallower water nearshore cools to lower temperatures during winter and heats more rapidly during spring and summer. While temperature gradients control lake flow patterns near the coast in summer, these temperature gradients are primarily created by variations in

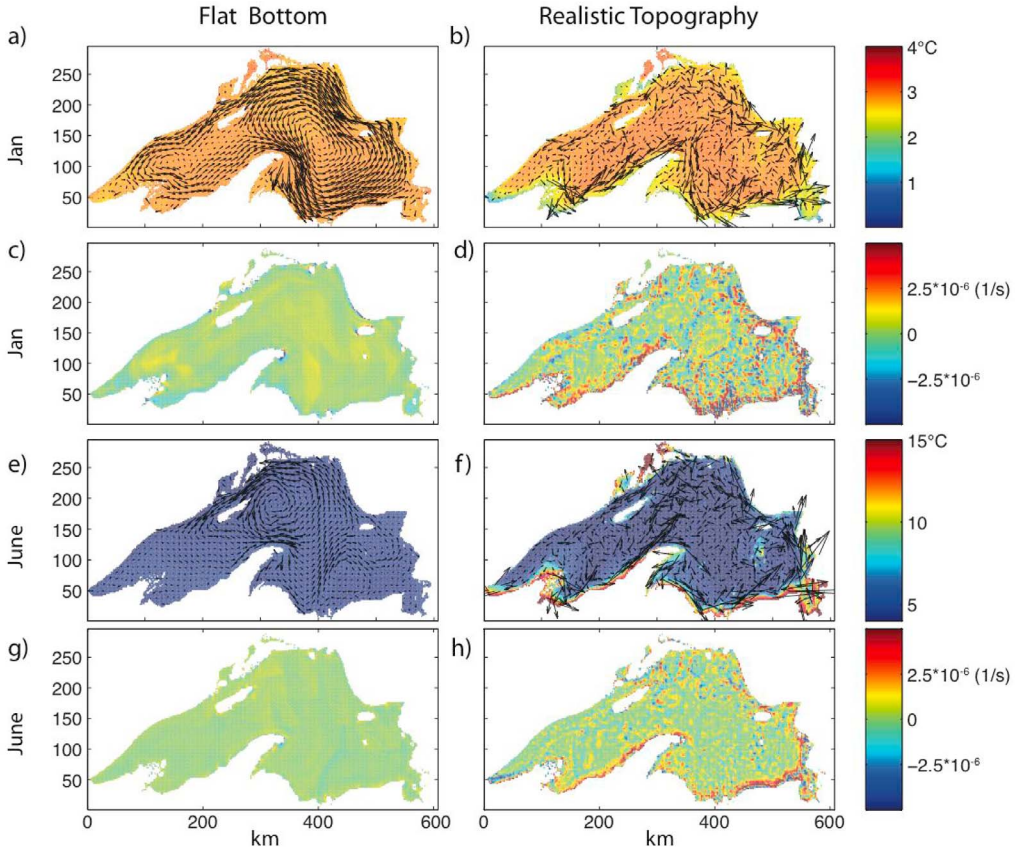

Figure 9. (a and b) Lake-wide depth-average currents and temperature in January 2006 for model simulations (a) with and (b) without realistic bathymetry. Color indicates temperature. (c and d) Depth-average vorticity during January for the uniform and realistic topography runs. (e and f) Depth-average currents and temperature during June and (g and h) vorticity for the uniform and realistic topography simulations.

lake bathymetry. In the open lake, wind is the largest driver of lake flow patterns and speeds. However, bathymetry creates small-scale structures in the open lake flow pattern as a result of a barotropic response to changes in depth, and local currents are not homogeneous as in the uniform bathymetry model run. The large gyre that encompasses the central and eastern basin in the uniform bathymetry run is split into two cyclonic gyres by the presence of bottom topography (Figure 9). In summary, winds are an important mechanism to circulation patterns year-round, and baroclinic effects alter nearshore currents during summer. Topographic gradients enhance horizontal temperature gradients during summer, split a single cyclonic gyre into two cyclonic gyres, and create small-scale structures in local flows throughout the year.

3.3. Trends

[39] Figure 10 shows annual average modeled depth-average temperature (analogous to heat content from zero degrees), surface temperature, depth average speed, surface current speed, and modeled summer mixed layer depths. Figure 10 also shows model forcing of air temperature, ice cover, and wind speed (10 m) over the lake during the same period. Slopes of trend lines and their p values are presented in Table 1. Modeled annual average depth-average temperature increased from 5.2°C (mean 1979–2003) to 5.5°C (mean 2002–2006). Lake surface temperatures increased from 7.4 to 8.1°C, forced by an increase in annual atmospheric temperature above the lake of 3.7 to 5.7°C. Modeled temperature trends likely underestimate realistic trends, given the warm bias in the forcing that causes the model to fail to capture the coldest observed temperatures but capture temperatures during the warmest years.

[40] As above lake air temperatures have increased [*Austin and Colman*, 2007], so have observed wind speeds above the open lake [*Desai et al.*, 2009]. Wind speeds increased from 4.9 (1979–1983) to 5.5 m/s (2002–2006) in the NARR forcing over the 28 year period, a rate comparable to observations. The increase in wind speed and lake surface temperature drives an increase in the wind stress on the lake, resulting in increased current speeds. Surface current speeds (15 m) increased from 4.1 to 5.2 cm/s. Mixed layer depths are determined by surface heating and turbulent mixing, often driven by the winds. The increase in lake temperatures could result in a shallowing of the thermocline, but an increase in wind stress should work to deepen the mixed layer. These two drivers appear to work against each other during the 28 year period; although wind speed is increasing over the lake, so is lake surface temperature, and

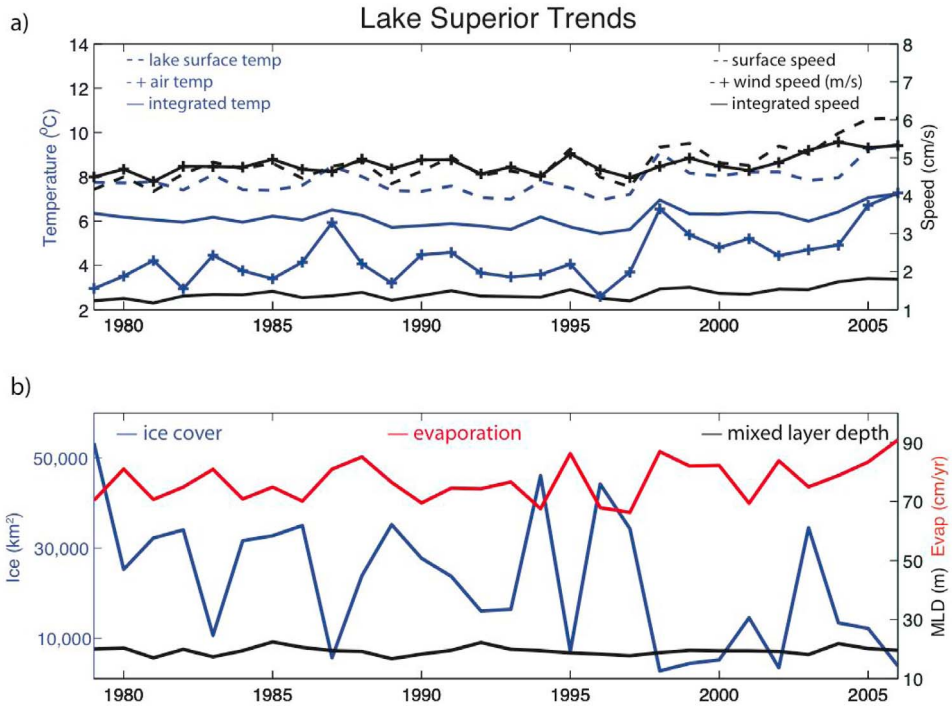

Figure 10. Lake-wide annual average modeled lake surface temperature, column-average temperature, surface current speed, depth-average current speed, and NARR 10 m above lake air temperature and wind speed from 1979 to 2006.

the modeled result is no statistically significant trend in mixed layer depth.

[41] Correlations between atmospheric conditions and lake response are shown in Table 2. Decreases in ice cover are significantly correlated to increases in air temperature ($r^2 = 0.52$) and modeled evaporation ($r^2 = 0.55$). Lake ice coverage is decreasing by 886 km^2/yr, but evaporation has no significant trend. Increases in wind speed also appear to contribute to increases in evaporation ($r^2 = 0.30$).

4. Discussion and Conclusions

[42] In this study, we use an eddy-resolving model to simulate and analyze the circulation of Lake Superior for 1979–2006. We find that summer surface circulation is highly organized with strong counterclockwise flows around the coastlines. This pattern is in agreement with the first map of Lake Superior circulation created by *Harrington* [1895] after a bottle drifter experiment. Flows are baroclinic during summer, and open lake subsurface flows follow along the isobaths, causing depth-average currents to consist of two cyclonic cells, strong coastal currents, and weak anticyclonic rotation near the St. Louis River. Circulation during winter is more barotropic, and depth-average flows consist of two rough cyclonic cells in the central and eastern basin and weaker coastal currents.

[43] By correlating anomalies in wind stress to anomalies in lake currents, we show that winter lake-wide circulation is primarily controlled by wind. Temperature gradients control currents nearshore in summer, while changes in open lake currents are wind driven all year. It has long been conjectured why medium to large-sized lakes are consistently cyclonic. This study agrees with the findings in Lake Michigan of *Schwab and Beletsky* [2003] that curl in the wind stress field is the dominant source of lake-wide positive vorticity. Lake Superior is warmer than the

Table 1. Lake Trends and p Values

Lake Characteristic	Trend	p Value
Lake surface temperature	0.34°C/decade	0.027
Heat content	0.12°C/decade	0.13
Ice cover (JFMA)	−886 km^2/yr	0.007
Speed (15 m)	0.37 cm/s/decade	0.0001
Speed (depth average)	0.13 cm/s/decade	0.0002
Above lake air temperature	0.8°C/decade	0.001
Wind speed	0.18 m/s/decade	0.002
Mixed layer depth	0.4 m shallower/decade	0.33
Evaporation	1.3 cm/decade	0.38
Buoy temperatures (AMJJASON)	0.7°C/decade	0.13

Table 2. The r^2 Values of Lake Variables of Interest

Variable 1	Variable 2	r^2
Speed (15 m)	wind speed	0.77
Speed (15 m)	speed (depth average)	0.98
Lake surface temp	air temp	0.81
Lake surface temp	ice cover	0.37 (r = −0.58)
Lake surface temp	heat content	0.88
Air temp	ice cover	0.52
Air temp	wind speed	0.26
Evaporation	ice cover	0.55 (r = −0.78)
Evaporation	wind speed (10 m)	0.30
Evaporation	lake surface temp	0.33
Lake surface temp	mixed layer depth	0.28
Wind speed	mixed layer depth	0.06 (r = −0.25)

surrounding land during winter, causing a mesoscale low-pressure system over the lake [*Petterssen and Calabrese*, 1959], which creates positive vorticity in the wind stress and promotes the cyclonic lake circulation. Due to the effect of lake surface temperatures on atmospheric stability and the presence of horizontal temperature gradients in the lake, even a spatially uniform wind field exerts wind stress with positive vorticity during summer. This effect, proposed by *Emery and Csanady* [1973], enhances thermally driven currents and captures the pattern of lake-wide circulation, but not speed (section 2 of Text S1 and Figure S6). The winter pattern of the circulation cannot be generated without spatially heterogeneous winds.

[44] From a uniform bathymetry run, we determine that lake bathymetry causes significant near to offshore temperature gradients that drive coastal currents during summer. Lake topography creates local heterogeneities in flow and confuses the depth-average large-scale circulation pattern year-round. East of Isle Royal, lake topography divides the single cyclonic gyre of the uniform bathymetry simulation into two, more complex cyclonic cells. While side-by-side gyres have been observed in Lake Ontario [*Pickett and Richards*, 1975] and many small lakes, the gyres were wind driven and counterrotating, not both cyclonic. Such counterrotating cells are sometimes present in the southwestern arm of Lake Superior. Both cells in central and eastern Lake Superior are cyclonic and are the result of a single cyclonic gyre divided by the spatially variable topography.

[45] We have shown that depth-average currents vary significantly within the summer season in both direction and speed, but that year-to-year changes in circulation at nine locations throughout the lake are minimal. *Waples and Klump* [2002] determined that wind directions have shifted over all of the Great Lakes except for Superior, so the lack of significant year-to-year variability during the modeled time period may not hold true in other Great Lakes. Still, Lake Superior is undergoing significant changes. Due to an increase in above lake temperature, modeled annual lake surface temperatures increase 1°C during the 28 year simulation, despite a known underestimate due to warm biases in the model forcing that are pronounced during cold years. *Austin and Colman* [2007] analyzed spring through summer buoy temperatures and determined that Lake Superior surface temperatures during this time of year are warming (1.21 ± 0.68°C/decade), twice as rapidly as regional air temperatures. For the lake to freeze, the entire water column must first cool to 3.98°C, and then the surface layer may begin to cool. Strong winter winds often make this surface layer very deep. Winter air temperatures determine lake ice coverage and spring lake heat content. A warmer winter leads to a larger spring heat content and an earlier onset of stratification, because less heat needs to be added to warm the entire water column to 3.98°C. This earlier onset of stratification leads to warmer lake surface temperatures throughout summer, causing a significant correlation between winter ice coverage and summer surface temperatures. Our findings are in agreement with *Austin and Colman* [2007].

[46] While *Hanrahan et al.* [2010] find an increasing trend in evaporation from GLERL modeling results in Lake Michigan and Lake Huron beginning in the 1980s, we do not find a statistically significant increase in evaporation in Lake Superior. The model indicates that ice cover is the dominant mechanism controlling annual evaporation. Lake surface temperatures and wind speeds are also increasing above the lake, but these changes are not large enough to cause a significant change in annual evaporation during this period.

[47] *Desai et al.* [2009] utilize observations and an atmospheric boundary layer model to show that wind speeds above Lake Superior increased during the model time period. They attribute this increase to the reduced air-lake surface temperature gradient observed by *Austin and Colman* [2007] that reduces atmospheric stability above the lake. The model responds to the increase in above lake wind speeds, causing an increase in modeled current speed. While an increase in wind speed alone would cool lake surface temperatures [*Huang et al.*, 2010], here consistent with observations, the increasing air temperature dominates. If the air-surface lake temperature gradient continues to decrease due to anthropogenic climate warming in the coming decades, we expect an increase in above lake wind speed, faster lake currents, and a decreased lake mixing time. These changes could spread pollutants and invasive species (mussels) more rapidly around the lake. Increased lake temperatures may also allow sea lampreys to begin feeding earlier in spring and thus to grow larger and more deadly to host fish [*Kitchell and Breck*, 1980] and may require updated management techniques. Increased and systematic year-round monitoring of lake thermal structure throughout the lake began in 2009 by investigators at the University of Minnesota-Duluth and the Large Lakes Observatory (J. Austin, personal communication, 2009) and will increase our understanding of the current, and likely future, physical state of the lake. These data and further numerical simulations can shed light on Lake Superior's physical and ecological response to climate change.

[48] **Acknowledgments.** The authors would like to thank NSF for funding (NSF OCE 0628560) and David Schwab at GLERL for providing meteorological observations over the lake for the 5 years (1997–2001) of alternative forcing. Noel Urban at Michigan Technological University graciously provided ADCP data from the KITES experiment for model evaluation. The authors also acknowledge Dierk Polzin at the University of Wisconsin-Madison for help with figures and two anonymous reviewers for their insightful comments. North American Regional Reanalysis data provided by NOAA/NESDIS/NCDC, Ashville, North Carolina, from their website (http://nomads.ncdc.noaa.gov/).

References

Anderson, W. G., A. Gnanadesikan, R. W. Hallberg, J. P. Dunne, and B. L. Samuels (2007), Impact of ocean color on the maintenance of the Pacific Cold Tongue, *Geophys. Res. Lett.*, *34*, L11609, doi:10.1029/2007GL030100.

Assel, R. A. (2003), An Electronic Atlas of Great Lakes Ice Cover Winters: 1973–2002, http://www.glerl.noaa.gov/data/ice/atlas/, Great Lakes Environ. Res. Lab., NOAA, Ann Arbor, Michigan.

Assel, R. A. (2005), Classification of annual Great Lakes ice cycles: Winters of 1973–2002, *J. Clim.*, *18*(22), 4895–4905, doi:10.1175/JCLI3571.1.

Austin, J. A., and S. M. Colman (2007), Lake Superior summer water temperatures are increasing more rapidly than regional air temperatures: A positive ice-albedo feedback, *Geophys. Res. Lett.*, *34*, L06604, doi:10.1029/2006GL029021.

Beletsky, D., and D. Schwab (2008), Climatological circulation in Lake Michigan, *Geophys. Res. Lett.*, *35*, L21604, doi:10.1029/2008GL035773.

Beletsky, D., J. H. Saylor, and D. J. Schwab (1999), Mean circulation in the Great Lakes, *J. Great Lakes Res.*, *25*(1), 78–93, doi:10.1016/S0380-1330(99)70718-5.

Chen, C. S., J. R. Zhu, E. Ralph, S. A. Green, J. W. Budd, and F. Y. Zhang (2001), Prognostic modeling studies of the Keweenaw current in Lake Superior. Part I: Formation and evolution, *J. Phys. Oceanogr.*, *31*(2), 379–395, doi:10.1175/1520-0485(2001)031<0379:PMSOTK>2.0.CO;2.

Desai, A. R., J. A. Austin, V. Bennington, and G. A. McKinley (2009), Stronger winds over a large lake in response to weakening air-to-lake temperature gradient, *Nat. Geosci.*, *2*(12), 855–858, doi:10.1038/ngeo693.

Dororstkar, A., L. Boegman, P. J. Diamessis, and A. Pollard (2010), Comparison of hydrostatic and non-hydrostatic modeling of internal wave fields in Cayuga Lake, paper presented at 53rd International Association of Great Lakes Research Conference, Int. Assoc. of Great Lakes Res., Toronto, Ont., Canada.

Dutkiewicz, S., M. Follows, and P. Parekh (2005), Interactions of the iron and phosphorus cycles: A three-dimensional model study, *Global Biogeochem. Cycles*, *19*, GB1021, doi:10.1029/2004GB002342.

Emery, K. O., and G. T. Csanady (1973), Surface circulation of lakes and nearly locked seas, *Proc. Natl. Acad. Sci. U. S. A.*, *70*(1), 93–97, doi:10.1073/pnas.70.1.93.

Hanrahan, J. L., S. V. Kravtsov, and P. J. Roebber (2010), Connecting past and present climate variability to water levels of Lakes Michigan and Huron, *Geophys. Res. Lett.*, *37*, L01701, doi:10.1029/2009GL041707.

Harrington, M. W. (1895), Surface currents of the Great Lakes, bulletin, Weather Bur., U.S. Dep. of Agric., Washington, D. C.

Huang, A., Y. R. Rao, and Y. Lu (2010), Evaluation of a 3-D hydrodynamic model and atmospheric forecast forcing using observations in Lake Ontario, *J. Geophys. Res.*, *115*, C02004, doi:10.1029/2009JC005601.

Kitchell, J. F., and J. E. Breck (1980), Bioenergetics model and foraging hypothesis for sea lamprey (*Petromyzon marinus*), *Can. J. Fish. Aquat. Sci.*, *37*(11), 2159–2168, doi:10.1139/f80-258.

Lam, D. C. L. (1978), Simulation of water circulations and chloride transports in Lake Superior for summer 1973, *J. Great Lakes Res.*, *4*(3–4), 343–349, doi:10.1016/S0380-1330(78)72203-3.

Large, W. G., J. C. McWilliams, and S. C. Doney (1994), Oceanic vertical mixing: A review and a model with a nonlocal boundary layer parameterization, *Rev. Geophys.*, *32*(4), 363–403, doi:10.1029/94RG01872.

Liu, W., and K. G. Lamb (2010), Internal Kelvin Waves in Lake Erie, paper presented at 53rd International Association of Great Lakes Research Conference, Int. Assoc. of Great Lakes Res., Toronto, Ont., Canada.

Marshall, J., A. Adcroft, C. Hill, L. Perelman, and C. Heisey (1997a), A finite volume, incompressible Navier-Stokes model for studies of the ocean on parallel computers, *J. Geophys. Res.*, *102*(C3), 5753–5766, doi:10.1029/96JC02775.

Marshall, J., C. Hill, L. Perelman, and A. Adcroft (1997b), Hydrostatic, quasi- hydrostatic, and nonhydrostatic ocean modeling, *J. Geophys. Res.*, *102*(C3), 5733–5752, doi:10.1029/96JC02776.

McKinley, G. A., M. J. Follows, and J. Marshall (2004), Mechanisms of CO_2 air-sea flux variability in the Equatorial Pacific and North Atlantic with implications for atmospheric inversions, *Global Biogeochem. Cycles*, *18*, GB2011, doi:10.1029/2003GB002179.

Mesinger, F., et al. (2006), North American regional reanalysis, *Bull. Am. Meteorol. Soc.*, *87*(3), 343–360, doi:10.1175/BAMS-87-3-343.

Petterssen, S., and P. A. Calabrese (1959), On some weather influences to warming of the air by the Great Lakes in winter, *J. Meteorol.*, *16*(6), 646–652.

Pickett, R. L., and F. P. Richards (1975), Lake Ontario mean temperatures and mean currents in July 1972, *J. Phys. Oceanogr.*, *5*(4), 775–781, doi:10.1175/1520-0485(1975)005<0775:LOMTAC>2.0.CO;2.

Prakash, S., J. F. Atkinson, and M. L. Green (2007), A semi-Lagrangian study of circulation and transport in Lake Ontario, *J. Great Lakes Res.*, *33*(4), 774–790, doi:10.3394/0380-1330(2007)33[774:ASSOCA]2.0.CO;2.

Querin, S., A. Crise, D. Deponte, and C. Solidoro (2006), Numerical study of the role of wind forcing and freshwater buoyancy input on the circulation in a shallow embayment (Gulf of Trieste, northern Adriatic Sea), *J. Geophys. Res.*, *111*, C03S16, doi:10.1029/2006JC003611.

Quinn, F. H. (1992), Hydraulic residence times of the Laurentian Great Lakes, *J. Great Lakes Res.*, *18*(1), 22–28, doi:10.1016/S0380-1330(92)71271-4.

Schwab, D. J., and K. W. Bedford (1999), The great lakes forecasting system, in *Coastal Ocean Prediction*, *Coastal Estuarine Stud.*, vol. 56, edited by C. N. K. Moores, pp. 157–173, AGU, Washington, D. C.

Schwab, D. J., and D. Beletsky (2003), Relative effects of wind stress curl, topography, and stratification on large-scale circulation in Lake Michigan, *J. Geophys. Res.*, *108*(C2), 3044, doi:10.1029/2001JC001066.

Schwab, D. J., and D. L. Sellers (1996), Computerized bathymetry and shorelines of the Great Lakes, *Data Rep. ERL GLERL 16*, 8 pp., NOAA, Ann Arbor, Mich.

Schwab, D. J., D. Beletsky, J. DePinto, and D. M. Dolan (2009), A hydrodynamic approach to modeling phosphorous distribution in Lake Erie, *J. Great Lakes Res.*, *35*(1), 50–60, doi:10.1016/j.jglr.2008.09.003.

Sheng, J. Y., and Y. R. Rao (2006), Circulation and thermal structure in Lake Huron and Georgian Bay: Application of a nested-grid hydrodynamic model, *Cont. Shelf Res.*, *26*(12–13), 1496–1518, doi:10.1016/j.csr.2006.01.019.

Sloss, P. W., and J. H. Saylor (1976), Large-scale current measurements in Lake Superior, *Tech. Rep. ERL 363-GLERL 8*, NOAA, Ann Arbor, Mich.

Smagorinsky, J. (1963), General circulation experiments with the primitive equations. Part I. The basic experiments, *Mon. Weather Rev.*, *91*(3), 99–164.

Urban, N. R., M. T. Auer, S. A. Green, X. Lu, D. S. Apul, K. D. Powell, and L. Bub (2005), Carbon cycling in Lake Superior, *J. Geophys. Res.*, *110*, C06S90, doi:10.1029/2003JC002230.

Waples, J. T., and J. V. Klump (2002), Biophysical effects of a decadal shift in summer wind direction over the Laurentian Great Lakes, *Geophys. Res. Lett.*, *29*(8), 1201, doi:10.1029/2001GL014564.

Williamson, C. E., J. E. Saros, and D. W. Schindler (2009), Lakes and reservoirs provide key insights into the effects and mechanisms of climate change, *Science*, *323*(5916), 887–888, doi:10.1126/science.1169443.

Zhu, J. R., C. S. Chen, E. Ralph, S. A. Green, J. W. Budd, and F. Y. Zhang (2001), Prognostics modeling studies of the Keweenaw current in Lake Superior. Part II: Simulation, *J. Phys. Oceanogr.*, *31*(2), 396–410, doi:10.1175/1520-0485(2001)031<0396:PMSOTK>2.0.CO;2.

V. Bennington and G. A. McKinley, Department of Atmospheric and Oceanic Sciences, University of Wisconsin-Madison, 1225 W. Dayton St., Madison, WI 53706, USA. (benesh@wisc.edu)

N. Kimura and C. H. Wu, Department of Civil and Environmental Engineering, University of Wisconsin-Madison, 1415 Engineering Dr., Madison, WI 53706, USA.